Temperature Dependence of Atomic-Scale Stick-Slip Friction

Lars Jansen,[1] Hendrik Hölscher,[2] Harald Fuchs,[1] and André Schirmeisen[1,*]

[1]*Physikalisches Institut and Center for Nanotechnology (CeNTech), Westfälische Wilhelms-Universität Münster, Wilhelm-Klemm-Strasse 10, 48149 Münster, Germany*

[2]*Karlsruhe Institute of Technology (KIT), Institute for Microstructure Technology, Hermann-von-Helmholtz-Platz 1, 76356 Eggenstein-Leopoldshafen, Germany*

(Received 11 March 2010; published 25 June 2010)

We report experiments of atomic stick-slip friction on graphite as an explicit function of surface temperature between 100 and 300 K under ultrahigh vacuum conditions. A statistical analysis of the individual stick-slip events as a function of the velocity reveals an agreement with the thermally activated Prandtl-Tomlinson model at all temperatures. Taking into account an explicit temperature-dependence of the attempt frequency all data points collapse onto one single master curve.

DOI: 10.1103/PhysRevLett.104.256101 PACS numbers: 68.35.Af, 07.79.Sp, 62.20.Qp, 68.37.Ps

Although friction is a familiar force from everyday life its physical origins are still under dispute. The first concept of microscopic friction was introduced by Prandtl [1] and Tomlinson [2] almost a century ago, who condensed the highly complex phenomenon of sliding friction into a simple atomistic model (PT model). Today it still receives widespread attention for the analysis of atomic-scale friction [3–7], including the phenomenon of superlow friction [8] and its external control [9]. Temperature plays an important role in the PT model leading for instance to a logarithmic velocity dependence [10] and the effect of thermolubricity [11]. However, the PT model predicts a strictly monotonic decrease of friction with increasing temperature which has been questioned recently [12]. Here we report experiments on true atomic stick-slip friction as an explicit function of surface temperature on graphite(0001). The logarithmic scaling of friction with velocity is found from ambient down to cryogenic temperatures. We propose a scaling of all friction-temperature values onto a master curve, accounting for a temperature dependent attempt frequency. This expands the validity of the fundamental PT-model description of friction phenomena to the influence of temperature.

The PT model is based on a mechanical picture where an atom attached via a spring to a moving top surface is sliding over the potential energy landscape of the bottom surface in the ''stick-slip'' mode (Fig. 1). The sliding atom sticks in a potential energy minimum until the lateral force of the spring is sufficient to induce a sudden jump into the neighboring minimum. In this case finite surface temperature will introduce a statistical element, such that jumps into the neighboring site become more likely already at lower lateral forces, leading to a monotonic decrease of friction with increasing temperature [see simulations in Fig. 1(c)]. A direct consequence of this thermally activated PT model is that friction scales with the logarithm of the sliding speed, which has been verified in numerous experiments and simulations [5,10,11,13].

Despite the undisputed success of the PT model some experiments yielded puzzling results when the influence of temperature was investigated [12,14]. For example, the friction-temperature curves for a nanoscopic silicon-silicon contact reveal a peaklike enhancement of friction at 100 K [14]. However, these results were recently explained by the collective behavior of randomly distributed multiple bonds at the tip-sample interface [15], in obvious contradiction to the PT model assuming a single tip atom in a periodic surface potential. On MoS_2 friction was observed to increase exponentially with decreasing temperature until 220 K with a crossover to athermal atomic wear processes below this threshold [12], again in contrast to the PT model. Considering these recent results, we must ask the following: Does the PT model fail because the model conditions are never sufficiently fulfilled in experiments or is this model simply inadequate to predict the influence of temperature on friction?

Here we report experiments on true atomic stick-slip friction as an explicit function of surface temperature for graphite(0001). In contrast to previously reported friction-temperature experiments [15], where large scan areas and rough samples prevented the explicit observation of atomic stick-slip friction, here we try to mimic the idealized PT-model geometry as close as possible. Therefore, we measured frictional forces of an atomically resolved stick-slip process for temperatures between about 100 and 300 K for a range of velocities under clean ultrahigh vacuum conditions. A logarithmic scaling velocity dependence is found from ambient down to cryogenic temperatures. We propose a scaling of all friction-temperature values onto a master curve, accounting for a temperature-dependent attempt frequency. This expands the validity of the fundamental PT-model description of friction phenomena to the influence of temperature.

The friction experiments were performed with a commercial atomic force microscope (AFM) integrated into an ultrahigh vacuum (UHV) chamber operated at a base pressure of 2×10^{-10} mbar (variable temperature

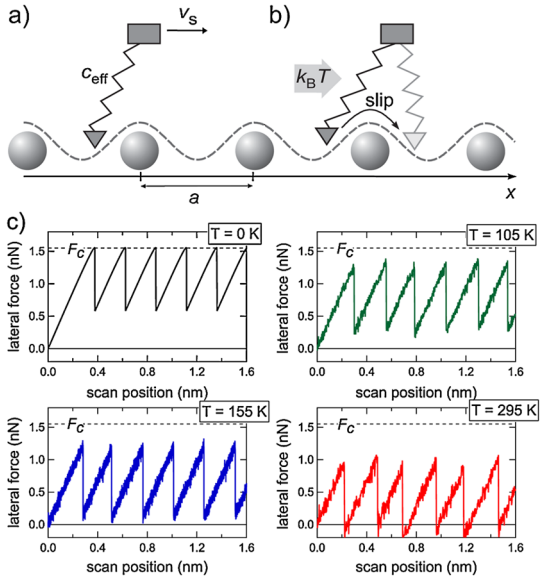

FIG. 1 (color online). (a) Atomic stick-slip friction in the thermally activated Prandtl-Tomlinson model can be explained with a mechanical model. An atom attached via a spring to a moving top surface is sliding over the potential energy landscape of the bottom surface (dashed line). (b) If the tip is scanned over the sample surface the spring elongates till its force is large enough to overcome the potential and the tip jumps into the next minimum. Thermal energy induces premature jumps, reducing the average slip-inducing lateral force. (c) Simulation of the stick-slip movement of the tip for different temperatures using the thermally activated PT model [13]. For $T = 0$ K the force $F_c = 1.55$ nN is needed to overcome the potential barrier. With increasing temperature, however, the tip jumps earlier and the lateral forces reduce. The assumed scan velocity of 125 nm/s corresponds to the experimental one in Fig. 3; all other parameters also correspond to the experimental ones described in the text.

AFM from Omicron Nanotechnology), which was used to quantify temperature-dependent friction on polymers before [16]. In this setup the sample temperature can be varied over a wide range, while the cantilever base stays at room temperature. As a sample we chose highly oriented pyrolytic graphite (HOPG) due to its known inertness to repeated scanning with the AFM tip. Shortly before the experiments the graphite sample was cleaved inside the UHV system. The force sensor was a single-crystalline rectangular silicon cantilever (LFMR-type by Nanosensors) of length 229 μm, width 43 μm, and with a silicon tip of height 14 μm. The normal- and torsional-spring constants of the cantilever were $c_n = 0.14$ N/m and $c_l = 12.7$ N/m, respectively. Friction forces were calibrated using the method described in Ref. [17].

Measurements were performed at room temperature first, and then from the lowest temperature obtained by liquid nitrogen ($T = 109$ K) in ≈ 50 K temperature intervals up to room temperature ($T = 295$ K) again. At each temperature, large areas of 100×100 nm^2 were scanned to identify flat terraces without any step edges. Then, the scan area was reduced to 3×3 nm^2, where the stick-slip friction was recorded in both, forward- and backward-direction as a function of the scan velocity ranging from 50 nm/s–1500 nm/s. The externally applied load was fixed at 30 nN throughout the whole experiment. The adhesion forces were obtained from the jump-off forces of several force-distance curves, giving a value of (15.0 ± 3.3 nN) independent of temperature [Fig. 2(d)].

Special care was taken to orient the sample surface such that the $[\bar{1}2\bar{1}0]$-direction of the (0001)-plane of HOPG was parallel to the fast scan-direction [18]. This is necessary to exclude artifacts arising from different crystal orientations [19] and also to minimize two-dimensional stick slip [3]. Figures 2(a) and 2(b) show representative lateral force maps at the lowest [$T = 109$ K, Fig. 2(a)] and highest [$T = 295$ K, Fig. 2(b)] investigated temperatures, verifying that the alignment was successful.

In the *stick* phase, the cantilever tip is confined to a local minimum of the surface potential, where a finite energy barrier prevents the tip from jumping into the next minimum. Once the cantilever is moved with a scan-velocity v, the lateral force increases according to Hooke's law with the effective spring constant c_{eff} describing the combined effect of elastic deformation of the cantilever and the contact region of the surface, while the tip remains in the given minimum. Because of the force increase, the effective energy barrier is reduced. At some point, where the energy barrier has not yet vanished, thermal noise will drive the tip to be released in a *slip*-phase jumping into the next potential minimum. Then, a new stick phase begins, leading to a characteristic sawtooth type motion.

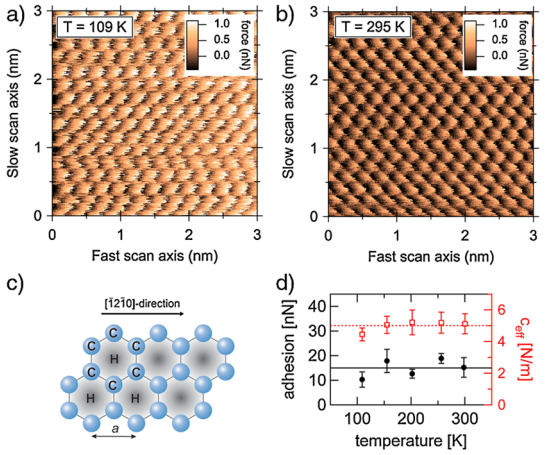

FIG. 2 (color online). Friction force experiments on HOPG showed atomic resolution from (a) 109 K up to (b) 295 K. These two lateral force maps have a size of 3×3 nm^2 and were acquired at a sliding velocity of $v = 125$ nm/s. (c) Schematic of the underlying structure of the graphite layer. The spheres indicate the single carbon atoms, arranged in a honeycomb pattern, in which the shaded areas, assigned with H, denote the hollow sites. (d) The adhesion (or snap-off) force (closed symbols) and the effective lateral contact stiffness (open symbols) reveal no systematic trend with temperature.

Figure 3 shows individual line profiles from experimental lateral force maps for the lowest, an intermediate and the highest investigated temperature from top to bottom, where this characteristic motion is clearly resolved. The sudden drops in the lateral force after a linear increase correspond to the slip events of the tip from one minimum site of the potential to the next. These minimum sites are located in the center of the hexagonal carbon rings of the surface structure [3] [Fig. 2(c)]. Friction maps for all temperatures and at all velocities show this characteristic sawtooth type pattern as predicted by the simulations in Fig. 1(c). None of the experimental friction scans showed multiple slip events, which can influence the temperature dependence of friction [20]. The observed average slip distance of 0.25 nm is in good agreement with the unit cell periodicity of the carbon lattice of $a = 0.246$ nm. The lateral contact stiffness c_{eff} was obtained from the linear force increase between two single slip events of the experimental stick-slip scan lines. The average value of $c_{\mathrm{eff}} = (4.95 \pm 0.34)$ N/m showed no systematic deviations for different temperatures [Fig. 2(d)]. Thus, these measurements satisfy all conditions necessary to mimic the PT-model situation of single step stick-slip friction at the atomic scale under temperature variation.

Owing to the statistical nature of the thermally activated jump processes the maximum lateral force F_l reached in the stick phase before the slip event varies significantly. Figure 3 demonstrates that on average, however, the jump inducing forces successively decrease with increasing temperature. For a quantitative analysis we extract the experimental slip-inducing force F_l^{exp} [see the arrows in Fig. 3(a)] from the trace and retrace lateral force maps [18]. Each map consisted of 400 single scan lines yielding about 10 000 individual force values per measurement. These were collected into force histograms [18]. Then the most probable slip-inducing force was determined from the peak force value $\tilde{F}_l^{\mathrm{exp}}$ at the maximum of these histograms. This procedure was applied to the friction maps at all measured velocity and temperature combinations. It is important to note that reproducible data was obtained only using the above described method of single jump analysis, while the commonly used simple averaging of friction loops resulted in much reduced data quality.

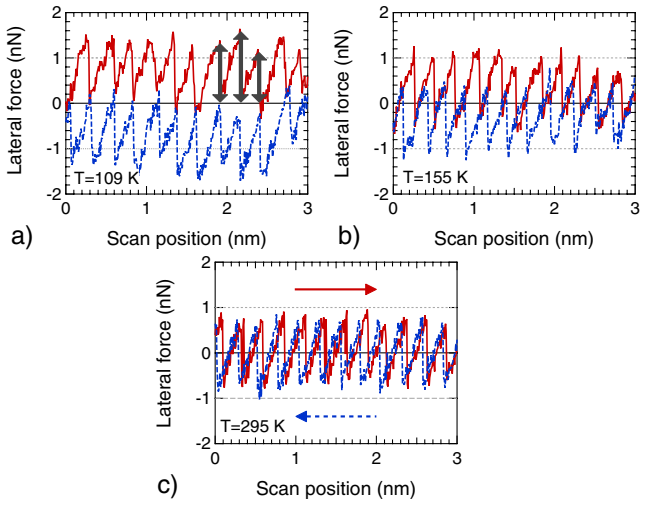

FIG. 3 (color online). Experimental atomic friction loops for different temperatures reveal the stick-slip movement in forward- (solid lines) and backward-direction (dashed lines), acquired at increasing temperatures: (a) 109, (b) 155, and (c) 295 K, respectively. The scan-velocity was $v = 125$ nm/s. The signals are offset and tilt corrected by an average over the whole friction-loop. The dashed lines indicate a force value of 1 nN for a better comparison between the graphs. The black arrows in (a) indicate the slip-inducing forces $\tilde{F}_l^{\mathrm{exp}}$, which were numerically determined for all jumps in the data sets.

The resulting friction-velocity isotherms are shown in Fig. 4(a) by symbols for all temperatures. Curves taken at room temperature before and after the low temperature measurements agree within the experimental uncertainty, thus verifying that the tip-sample interface suffered no permanent changes [21]. While friction generally increases with scan velocity, the slope and offset of the isotherms changes significantly with temperature. This result is in agreement with the thermally activated PT model, which predicts the following relationship between friction, temperature, and velocity [5,6,13,22]

$$F_l(v, T) = F_c - \left(\beta k_B T \ln\left(\frac{v_c}{v}\right)\right)^{2/3}. \quad (1)$$

The parameter

$$v_c = (2 f_0 \beta k_B T)/(3 c_{\mathrm{eff}} \sqrt{F_c}) \quad (2)$$

is a critical velocity with f_0 as the force free attempt rate.

The parameter F_c reflects the maximum slip-inducing force at zero temperature and should therefore be independent of the variation of temperature, as long as applied load and adhesion do not change during the experiments [5]. The factor β is a measure of the curvature of the potential energy corrugation, which is also independent of temperature. The attempt rate f_0, however, is known to depend on the actual temperature [23]. Therefore, we must allow that $f_0 = f_0(T)$ when comparing Eq. (1) to our experiments.

Assuming that the surface potential is sufficiently approximated by a sinusoidal shape an analytical relationship between β and F_c can be derived [5]

$$\beta_{\mathrm{sin}}(F_c) = (3\pi\sqrt{F_c})/(2\sqrt{2}a). \quad (3)$$

Experimentally derived values for β can differ from the ideal β_{sin} by an order of magnitude, since the real potential usually deviates from the perfectly sinusoidal shape [5]. Although we are very close to the idealized situation due to the well-oriented crystal and the observed equidistant stick-slip in the force maps, we allow a small factor δ of the order of 1 to account for those deviations $\beta_{\mathrm{sin}}^{(\delta)} = \delta \cdot \beta_{\mathrm{sin}}$.

The results of fitting the experimental data to Eq. (1) are shown as as dashed and solid lines in Fig. 4(a) where we explicitly considered the constraints given by

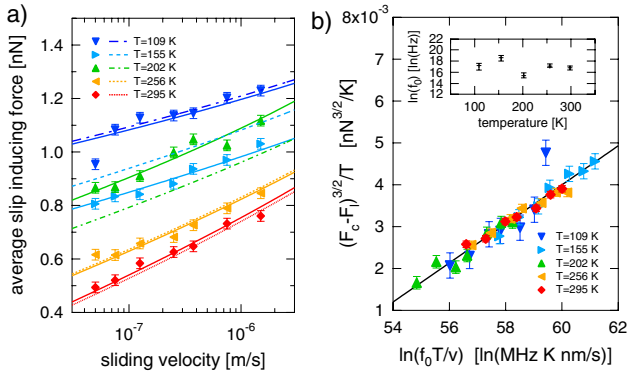

FIG. 4 (color online). (a) The measured slip-inducing forces are plotted by symbols as a function of sliding velocity for different temperatures. The dashed lines represent lines represent a fit to the data using Eq. (1) with f_0 fixed to 24 MHz for all temperatures. As described in the text the data fits much better if the temperature dependence is explicitly considered (solid lines). (b) The master curve based on all data sets. Plotting all experimental data in this way all measurements collapse into one linear curve. The inset shows a plot of the attempt rate $\ln(f_0(T))$ which is the only parameter varied in the fits shown by solid lines in (a).

Eq. (2) and (3). Best fits are achieved with $F_c = (1.60 \pm 0.05)$ nN and $\delta = (1.95 \pm 0.05)$ for all temperatures. The deviation of δ from unity indicates that the surface potential is indeed not perfectly sinusoidal. The effective energy barrier, however, can be estimated from $E_{0,\mathrm{sin}} = aF_c/\pi \approx 0.78$ eV [5,8] and still falls within the range of typical energy barriers for atomic-scale friction [5,8,18]. As discussed above the agreement of the PT-model with the data is much improved if we consider an explicit temperature dependence of the attempt frequency. To demonstrate this feature we contrast the fits for a fixed (dashed lines) and free (solid lines) attempt frequency in Fig. 4(a). The fit values for the logarithm of the free attempt rate $\ln(f_0(T))$ are ranging between 15.4 and 18.8 (i.e., between 5 and 120 MHz), depending on the sample temperature as shown in the inset in Fig. 4(b).

The experimental friction-velocity isotherms allow us to propose a scaling of all data sets onto one single master curve. In Fig. 4(b) we graphed all data sets as $(F_c - F_l)^{3/2}/T$ over $\ln(f_0(T)T/v)$, thus including the temperature dependence of the attempt frequency $\ln(f_0(T))$. As expected from Eq. (1) all data points follow a linear relationship in this plot diagram. So far [13,24] f_0 was not assumed to depend on temperature and master curves were graphed as a function of $\ln(T/v)$. However, only by considering the temperature dependence of the attempt frequency all data collapse into one single curve.

In Fig. 4(b) the variation of $\ln(f_0(T))$ essentially corresponds to a horizontal adjustment of the friction-velocity curves, while F_c influences the vertical shift. Since the effective tip load did not change significantly throughout the whole experiment, it is reasonable to keep F_c constant for all fits [5]. This leaves the attempt frequency f_0 as the only parameter that can depend on temperature. So far f_0 was related to the lateral resonance frequency of the tip-sample contact [5,8], as evidenced by the strong influence of an external mechanical excitation [9]. However, we find that this resonance point can show a temperature dependence not anticipated so far.

In summary, our experimental study reveals that the thermally activated Prandtl-Tomlinson model retains its validity under temperature variation, if the underlying idealized geometry is mimicked correctly, the statistical nature of the model is accounted for and an explicit temperature dependence of the attempt frequency is considered. This may seem surprising, considering the drastic simplifications of the model, like the one-dimensional surface potential and the single atom-on-spring geometry. However, it expands the validity of one of the most fundamental concepts of atomic friction, with comparably simple analytical solutions, to the variation of temperature. Our results should considerably help recent efforts to understand and describe the temperature dependence of friction as one of the most unexplored areas in nanotribology.

*schirmeisen@uni-muenster.de

[1] L. Prandtl, Z. Angew. Math. Mech. **8**, 85 (1928).
[2] G. A. Tomlinson, Philos. Mag. **7**, 905 (1929).
[3] H. Hölscher *et al.*, Phys. Rev. B **57**, 2477 (1998).
[4] H. Hölscher *et al.*, Phys. Rev. B **59**, 1661 (1999).
[5] E. Riedo *et al.*, Phys. Rev. Lett. **91**, 084502 (2003).
[6] H. Hölscher, A. Schirmeisen, and U. D. Schwarz, Phil. Trans. R. Soc. A **366**, 1383 (2008).
[7] H. Hölscher, D. Ebeling, and U. D. Schwarz, Phys. Rev. Lett. **101**, 246105 (2008).
[8] A. Socoliuc *et al.*, Phys. Rev. Lett. **92**, 134301 (2004).
[9] A. Socoliuc *et al.*, Science **313**, 207 (2006).
[10] E. Gnecco *et al.*, Phys. Rev. Lett. **84**, 1172 (2000).
[11] S. Y. Krylov *et al.*, Phys. Rev. E **71**, 065101(R) (2005).
[12] X. Zhao *et al.*, Phys. Rev. Lett. **102**, 186102 (2009).
[13] Y. Sang, M. Dubé, and M. Grant, Phys. Rev. Lett. **87**, 174301 (2001).
[14] A. Schirmeisen *et al.*, Appl. Phys. Lett. **88**, 123108 (2006).
[15] I. Barel *et al.*, Phys. Rev. Lett. **104**, 066104 (2010).
[16] L. Jansen *et al.*, Phys. Rev. Lett. **102**, 236101 (2009).
[17] P. Bilas *et al.*, Rev. Sci. Instrum. **75**, 415 (2004).
[18] A. Schirmeisen, L. Jansen, and H. Fuchs, Phys. Rev. B **71**, 245403 (2005).
[19] J. Y. Park *et al.*, Science **309**, 1354 (2005).
[20] Z. Tshiprut, S. Zelner, and M. Urbakh, Phys. Rev. Lett. **102**, 136102 (2009).
[21] See supplementary material at http://link.aps.org/supplemental/10.1103/PhysRevLett.104.256101 for experimental friction-velocity curves before and after the cooling cycle.
[22] B. N. J. Persson *et al.*, Wear **254**, 835 (2003).
[23] M. Evstigneev and P. Reimann, in *Fundamentals of Friction*, edited by E. Gnecco and E. Meyer (Springer, New York, 2006), Chap. 7, p. 117.
[24] S. Sills and R. M. Overney, Phys. Rev. Lett. **91**, 095501 (2003).